Doi: 10.32592/jorar.2022.14.1.2

Analysis of Temperature Change Properties in Tehran Using Satellite Data

Mohammad Javad Barati[1], Manuchehr Farajzadeh Asl[2], Reza Borna[3]

Date of submission: 10 Mar. 2021 *Date of acceptance: 12 Sep. 2021*

Original Article

Abstract

INTRODUCTION: The dearth of data and accurate climate information has made it difficult to study the relationship between human health and climate change. To study the surface heat island in the urban areas, land surface temperature must be calculated, and since no space sensor is capable of frequent thermal imaging at the required spatial resolution for urban studies, this study aimed to propose a method for urban temperature changing characteristics, and provide the results to the city managers and officials in health domains.

METHODS: SADFAT temporal and spatial integration model was used to prepare the data. Following that, changes in the spatial and temporal pattern of surface temperature data in Tehran were studied using exploratory methods of spatial data analysis, and the results were evaluated by classical statistical methods (normalization process, classification, and comparison of temperature classes of images). The heat island ratio index was employed to investigate the temporal changes in the intensity of the heat island.

FINDINGS: Temporal changes in the ratio of heat island in Tehran during 2017 showed that from the Julian days 1 to 81 (January 12 to April 2), as well as 153 to 281 (June 12 to October 16), the value of the intensity of the heat island in Tehran was higher than the average (about 0.067) due to changes in vegetation, climate, and air pollution, for 210 days in a year.

CONCLUSION: The diagram of periodic and irregular fluctuations of thermal islands showed that it was not logical to compare the spatial pattern of thermal islands without considering the time of location. These daily and weekly fluctuations in the intensity of the heat island, as well as the human exposure to it, cause a wide range of diseases, such as hypothermia, heatstroke, as well as cardiovascular and respiratory diseases, which consequently lead to death.

Keywords: Human Health; Thermal Island; Temporal and Spatial Integration.

How to cite this article: Barati MJ, Farajzadeh Asl M, Borna R. **Analysis of Temperature Change Properties in Tehran Using Satellite Data.** Sci J Rescue Relief 2022; 14(1): 10-18.

Introduction

The most obvious human impact on climate is the phenomenon of "urban heat island" on the local and regional scale (1). Even a single building complex shows a microclimate difference in relation to a flat plot of land in its natural state. A rise in the local temperature is closely related to human well-being and the use of urban energy, and due to the increasing need for energy, it leads to global climate change and affects humans. Among the consequences of climate change on human health, one can refer to cancer, mortality, diseases related to heart, asthma, allergies, respiratory and airborne diseases, cardiovascular diseases, stroke and neurological disorders, mental health disease, stress-dependent diseases, infectious and insect-borne diseases, as well as congenital diseases. In 2018, Hajizadeh et al. investigated the effects of climate change on human health and concluded that climate change was related to social, health and psychological issues and was a threat to health and mental health. The impact of climate

1- PhD Candidate in Satellite Meteorology, Science and Research Branch, Islamic Azad University, Tehran, Iran
2- Professor, Department of Physical Geography, Tarbiat Modares University, Tehran, Iran
3- Associate Professor, Department of Geography, Ahvaz Branch, Islamic Azad University, Ahvaz, Iran
Correspondence to: Manuchehr Farajzadeh Asl, Email: farajzam@modares.ac.ir

change on health is greater in low-income countries where there is a weak capacity to accept this phenomenon; however, this problem has also been observed in most vulnerable groups in developed countries (2).

In 2019, Sanagar et al. investigated the Effects of Urban Heat Islands Mitigation on Human Health through Changes in Urban Form in the Hot and Arid Climate of Mashhad. The findings indicated that the higher ratio of height to width led to less access of sunlight to the environment, and as a result, the ambient temperature decreased. Moreover, shading due to height to width ratio, and the presence of plants and wind in urban valleys can reduce the ambient temperature. In addition, the reduction of impermeable surfaces of urban coatings and the presence of materials with a high albedo, increase evapotranspiration, which provides cooling conditions for urban environments and reduces the adverse effects of urban heat on human health (3).

Therefore, all phenomena, including humans, are threatened by fluctuations in ambient temperature. However, due to the dearth of research/data and climate information with high accuracy, it seems difficult to study the relationship between human health and climate change; accordingly, it is necessary to estimate the urban heat islands and their variability in different days of the year. In order to obtain this information, this study utilized satellite data, temporal and spatial integration methods, and spatial analysis. The surface urban heat island is revealed by calculating the Land Surface Temperature (LST), which is obtained using thermal infrared remote sensing (TIR) data. The first studies attempting to investigate the urban thermal landscape using TIR data utilized AVHRR (a sensor installed on NOAA satellite) (Roth et al., 1989; Gallo and Owen, 1998; Streutker, 2003) (4-6). The spatial resolution of the thermal run for all these studies was 1.1 km, which was only suitable for preparing a large-scale map of the city temperature. Later, thermal infrared data of the Landsat TM, ETM +, and ASTER, with spatial resolutions of 120, 60, and 90 m, respectively, made it possible to extract the land surface temperature and study the urban heat islands more closely (Lu and Weng, 2006; Córdova, 2009) (7, 8).

Essa et al. (2013) used the radiometric surface temperature separation method, which was first employed as a method for temperature detection of agricultural areas, and then for the micro scale exponential thermal data of Landsat 7 to 30 meters for an urban area (9). Although these methods were successful, they did not provide sufficient frequent observations to monitor the urban climate. Most of the studies of urban heat islands with remote sensing technology conducted in Iran have considered the relationship between changes in land cover and Spatio-temporal dynamics of land surface temperature. Sadeghinia (2012), in his dissertation, studied the Spatio-temporal changes of the heat island of Tehran using Landsat TM multi-time images. The results showed that from 1986 to 2010, the amount of spatial autocorrelation of surface temperature increased, and the temperature variable tended to be more concentrated and clustered in space (10). In general, the studies on the heat island of Tehran show that valuable research has been conducted in this regard so far. Most investigations aimed to determine the spatial boundary of the heat island in Tehran, and most of them have been performed using a thermal image. Some of these studies have sought to introduce appropriate algorithms to extract the surface temperature of Tehran, and others have studied the role of land use in the thermal model of Tehran using a thermal image. However, since the heat island has periodic and irregular fluctuations and daily changes in land surface temperature are different due to land use/cover in different climatic conditions, there have been no studies so far to determine the daily surface temperature changes with a spatial accuracy of 30 meters using the satellite data. Therefore, this study provides city managers and health officials with the characteristics of temperature change in Tehran by separating pixel-based temperature with high spatial and temporal resolution.

Methods

Tehran is located on longitude 51°26′ to 51°33′ E and latitude 35°36′ to 35°46′ N. According to the comprehensive plan of 2006, the area of Tehran is about 611 square kilometers, and the population of Tehran according to the latest census of the National Statistics Center in 2016 is 8,693,706. This applied descriptive-analytical study calculated the daily land surface temperature in Tehran utilizing 22 Landsat 8 images with a resolution of 30 meters for reflective bands and 100 meters for thermal bands

[DOI: 10.32592/jorar.2022.14.1.2]

10 taken from the https://earthexplorer.usgs.gov and 365 MODIS products (MOD011A1) with a resolution of 1000 meters related to 2017 taken from http://modis.gsfc.nasa.gov

In order to achieve the pattern of Spatio-temporal changes of the heat island, reliable data must be initially available. However, no space sensor can provide frequent thermal imaging at the spatial resolution required for urban studies. Therefore, temporal-spatial integration methods are used to improve the spatial resolution of an image with high temporal resolution. This study employed the Spatio-temporal Adaptive Data Fusion Algorithm for Temperature mapping (SADFAT) model to apply the spatial-temporal properties of Operational Land Imager (OLI) and Moderate-Resolution Imaging Spectroradiometer (MODIS) images to estimate LSTs in urban areas. The data entered the model include thermal radiance of MODIS and Landsat images, as well as red and infrared bands near Landsat to predict the surface temperature of consecutive days in Tehran during 2017. This method uses two pairs of MODIS and Landsat images at the same time, as well as a set of MODIS images at the prediction time. Following that, the determination of the conversion coefficient of thermal radius changes of heterogeneous MODIS pixels to Landsat pixels increases the accuracy of prediction in the heterogeneous regions. All steps in the SADFAT model were coded in MATLAB software; moreover, the Landsat and MODIS data were read. The steps for implementing the model are given in the flowchart below.

Two perspectives were used to study the spatial and temporal changes of the heat island of Tehran. Initially, the changes in the spatial and temporal pattern of surface temperature data in Tehran were studied using exploratory spatial data analysis (Local Moran Method). Subsequently, using classical statistical methods (normalization process, classification, and comparison of temperature classes of images), the results of the Local Moran Method were evaluated.

Analysis of local spatial autocorrelation (The local Moran's I statistic)

The local Moran's I spatial autocorrelation statistic was used to determine the spatial pattern of local differences. This index measures the spatial difference of temperature values between each cell and adjacent cells and evaluates its significance. For cell *i*, the local Moran's value is calculated using the following equation (11):

Equation (1): $I_i = x_i \sum_{i=1, j \neq i}^{N} w_{ij}\ x_j$

Where N is the number of cells (spatial observations), x_i and x_j signify the standard observed values of cells i and j, respectively. w_{ij} presents the standardized amount of spatial weight, and the sum of the weights is 1. Similar to the general Moran's statistics, the results of the local Moran's statistics can be tested with Z scores. A confidence level is determined, if cell *i* has a positive value (i.e., I_i is a positive number), and the temperature value of cell *i* is similar to the temperature value of the adjacent cells. If the value of I_i is a large positive number, it indicates a strong clustering range.

On the other hand, if the value of I_i is negative and significant, the surface temperature value of cell *i* is very different from that of the adjacent cells, which indicates a negative spatial correlation. After the implementation of the local Moran's statistic, a significant map of local Moran was created. Local clusters and their types were identified using this map. In addition, the Moran scatter diagram helped determine the type of spatial autocorrelation that exists between locations. In this diagram, two groups of data were observed:

High-high points: Points that have a high temperature and are surrounded by high-temperature points. Hot clusters (heat islands) were identified according to the distribution of these points.

Low-low points: Due to the distribution of these points, cool clusters (a cool island or cool islands) were identified.

Temporal changes in the surface temperature data distribution pattern

In order to evaluate the results of exploratory spatial data analysis (local Moran), surface temperature data of Tehran were analyzed using statistical methods. Due to the fact that the studied images have daily, monthly, and seasonal changes, a direct comparison of the absolute temperature data extracted from the images is not logical and scientific. Therefore, the following equation was used to normalize the images (12).

Equation (2): $N_i = \frac{T_i - T_{min}}{T_{max} - T_{min}}$

[DOI: 10.32592/jorar.2022.14.1.2]

Table 1. Classification of the surface temperature data of the studied images

Temperature classification	Ranges related to each temperature class
Very low temperature (1st class): Very cool areas	$T \leq T_{mean}$- 1.5 std
Low temperature (2nd class): Cool areas	T_{mean}- 1.5 $std < T \leq T_{mean}$- std
Moderate temperature (3rd class): Moderate temperature areas	T_{mean}- $std < T \leq T_{mean}$+ std
High temperature (4th class): Warm areas	T_{mean}+ $std < T \leq T_{mean}$+ 1.5 std
Very high temperature (5th class): Very hot areas	$T > T_{mean}$+ 1.5 std

Where N_i is the normalized value of cell i, and T_i signifies the absolute temperature of cell i. moreover, T_{min} presents the minimum temperature of each image, and T_{max} indicates the maximum temperature of each image. The normalized images were then divided into five temperature classes using their mean±SD (7). In Table 1, T_{mean} is the mean temperature of each normalized image, and std signifies the standard deviation of each normalized image.

After classifying the surface temperature data of each image, the area of each temperature class was calculated in Arc GIS. Regarding the trend of the temporal changes, the area of each class was examined to determine the increasing or decreasing trends of each temperature class. Among the temperature classes of the above table, the temporal changes of the 1st and 5th classes show the very cool and very hot areas of Tehran, respectively, and are of significant importance. This part of the analysis identifies the changes in the pattern of a statistical distribution of surface temperature in Tehran on different days of the year; accordingly, the area of very hot areas (the hottest parts of the city) is obtained during a year.

Temporal changes of the heat island intensity

The Urban heat island Ratio Index (URI) was used to study the changes in the intensity of the heat island of Tehran. In this method, the data were initially normalized using *Equation* (2), and then the area and class of each temperature were calculated using the method presented in Table 1. *Equation* 3 shows the estimation of the heat island ratio index (13):

$$\textit{Equation}\ (3):\ \mathrm{URI} = \frac{1}{100m}\sum_{i=1}^{n} w_i p_i$$

Where URI is the heat island ratio index and m signifies the number of normalized temperature classes. In this study, the number of classes is shown by N presenting the number of temperature classes higher than the average (normal) temperature class. In this study, the 4th and 5th classes have higher temperatures, compared to the 3rd class that shows the average temperature. Accordingly, n is equal to 2, and w_i signifies the weight of the temperature classes that are higher than normal. According to the number of each class, numbers 4 (high temperature) and 5 (very high temperatures) were assigned to the 4th and 5th classes, respectively. p_i is the ratio of the area of temperature classes higher than normal to the total area of the city. To obtain this parameter, the area of each of the 4th and 5th classes is divided by the total area of the city; following that, the obtained number is multiplied by 100.

Findings

Visual evaluation of the predicted surface temperature images shows the good accuracy obtained from the application of the SADFAT integration method and the use of Landsat and MODIS thermal images. Furthermore, the temperature range difference between the maximum and minimum values of the predicted and observed Landsat surface temperatures is almost the same. Figure 1 illustrates one of the daily image outputs.

Local spatial autocorrelation (local Moran)

Figure 2 depicts the temporal changes in the number of high-high points related to the surface temperature. According to this figure, the high-high points in 2017 initiated to increase from Julian day of 105 (April 26) with 613,698 cases, to reach a maximum on 257 Julian day (September 23) with 668,613 cases. Expanded hot clusters are also observed up to 289 Julian days (October 24) with 642,374 cases, which then decreased rapidly.

The trend of temporal changes in the low-low points can be observed in Figure 3. During the study period, on days when the number of high-high points increased, a decrease was noted in the number of low-low points. Local spatial

[DOI: 10.32592/jorar.2022.14.1.2]

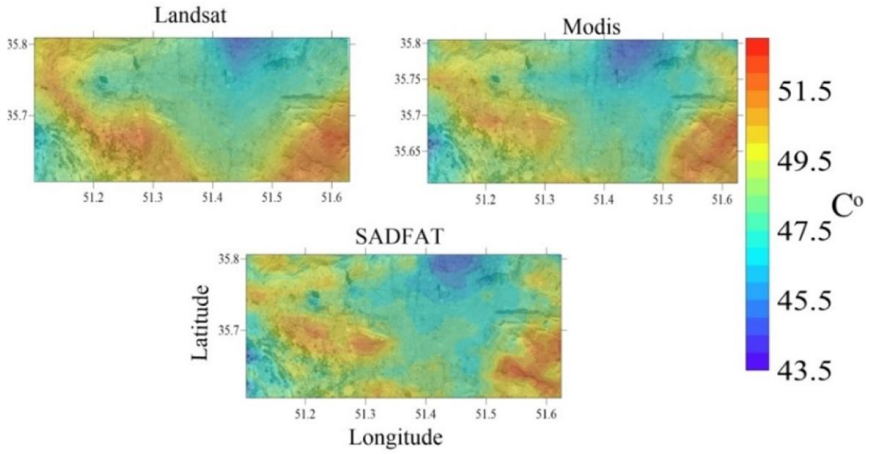

Figure 1. Land temperature images of Landsat and MODIS (July 4, 2017) (Celsius)

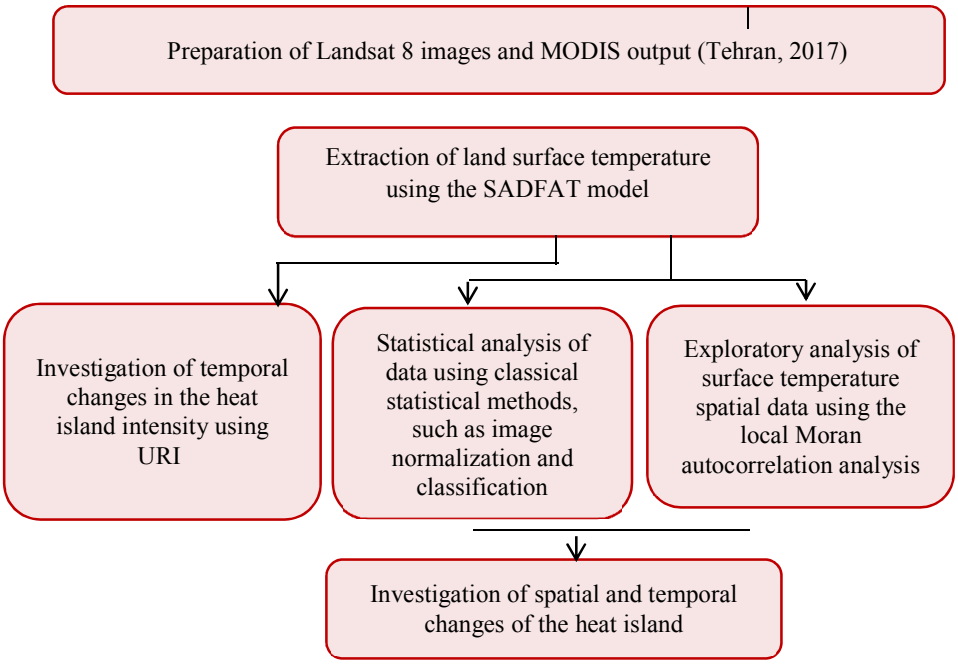

Figure 2. Research procedures

autocorrelation analysis by comparing Figures 2 and 3 shows that during the time interval of 105 to 289 Julian days (April 26 to October 15) when the hot clusters have expanded and strengthened, in contrast, the number of cool clusters has weakened and limited. Therefore, according to the obtained results, it can be stated that Tehran is faced with the expansion and intensification of the heat island effect these days.

Local Moran statistics not only identify the spatial changes of the heat island of Tehran on different days but also indicate the location and expansion of the heat island and the presence of new hot clusters every day of the year. The interpretation of the heat island condition identifies the location of the island on different parts and the relationship with the application types. The distribution of high-high points in all images in Tehran during 2017 shows the location of the heat island in the west on Districts 9, 21, and 22 and the western half of District 18. The study of the spatial

[DOI: 10.32592/jorar.2022.14.1.2]

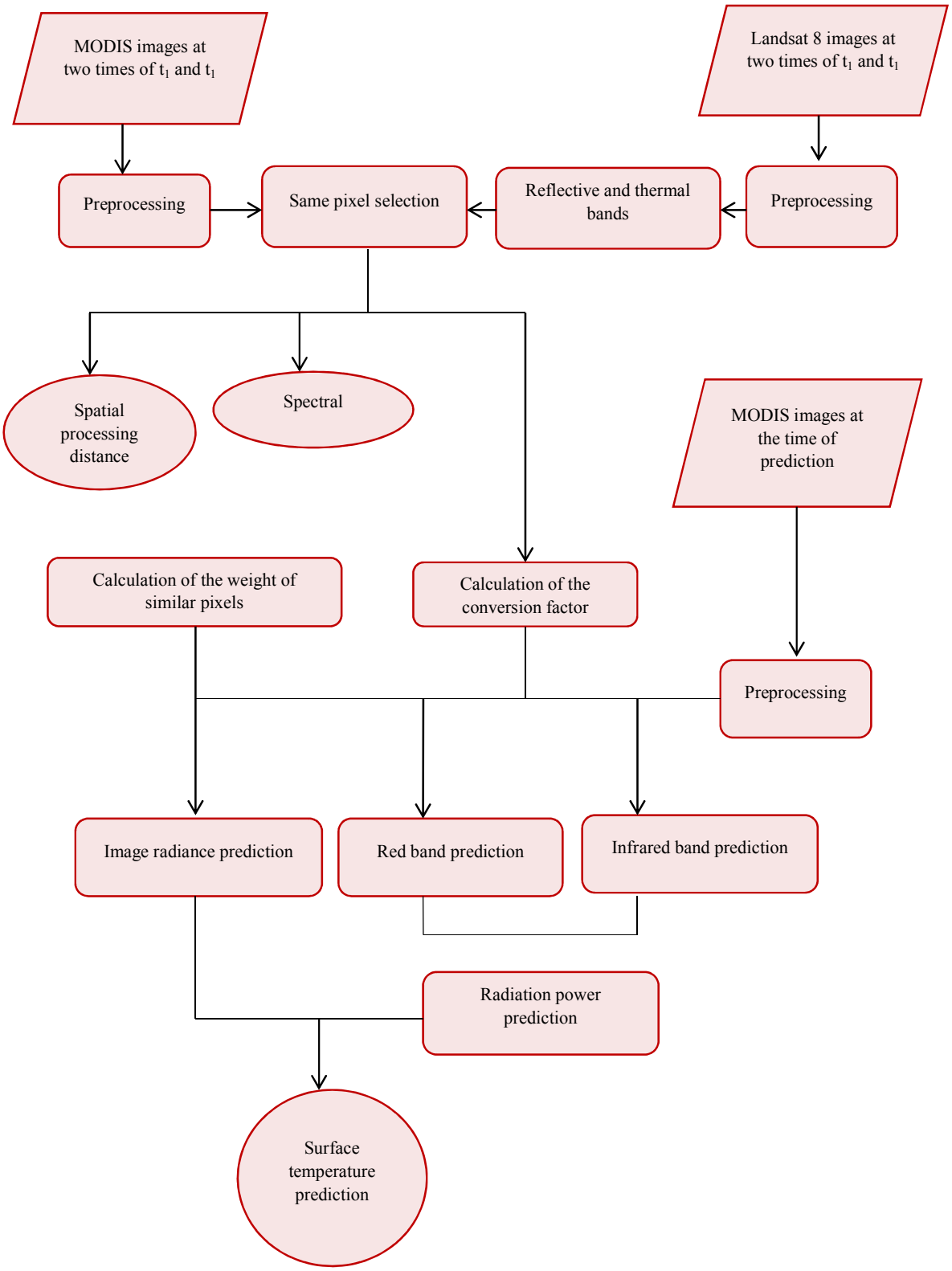

Figure 3. Flowchart of SADFAT model implementation

[DOI: 10.32592/jorar.2022.14.1.2]

Table 2. Area of temperature classes of thermal images of Tehran

Temperature Classification Julian Day	Class 1 Area Very low temperature (square kilometers)	Class 2 Area Low temperature (square kilometers)	Class 3 Area Moderate temperature (square kilometers)	Class 4 Area High temperature (square kilometers)	Class 5 Area Very high temperature (square kilometers)
1	45.5	110.9	237.2	147.2	63.4
49	66.6	120.8	240.4	113.6	62.8
73	60.1	111.7	238.9	125.3	68.2
105	83.4	136.0	250.6	80.3	53.9
145	45.9	90.9	305.2	114.2	48.0
169	27.6	73.4	317.9	101.6	83.7
201	44.7	134.3	245.2	93.8	77.2
233	42.4	133.8	250.4	103.8	73.8
257	48.5	126.6	254.2	107.5	67.4
289	50.5	142.0	239.8	98.1	73.8
313	74.0	180.0	209.2	70.0	71.0
365	96.0	149.0	219.2	89.0	51.0

range of low-low points in this year shows the location of a cool island in the northern parts of Tehran on Districts 1 and 3, and some parts of Districts 2 and 4. In all images of District 1, Municipality of Shemiranat was the coldest urban area of Tehran, and other cool clusters scattered throughout the city were located in the open and green spaces of Tehran.

Statistical analysis of surface temperature data in Tehran

Table 2 summarizes the area of each of the surface temperature classes of Tehran in square kilometers.

Investigation of the increasing or decreasing trends of five temperature classes during the study period showed that, in general, between Julian days 156 and 257 (June 15 to September 14), in contrast to the areas with very cool and cool temperatures (1st and 2nd classes), in which the areas have decreasing trend, the areas of classes with moderate and very high temperature (classes 3 and 5) have increased. The main hot cluster is located on Mehrabad Airport all year and has a very high surface temperature in all images. Furthermore, it is strengthened on the 169th Julian day (June 28) and has the greatest expansion in the west and southwest of Tehran. A strongly interconnected cluster remains until 313th Julian day (November 18), and then the clusters are scattered in the same areas with a smaller expansion. Figures 4 and 5 show the spatial distribution of temperature zones in Tehran on 169th (June 28) and 361st (January 6) Julian days in 2017, respectively. Temperature ranges 4 and 5 marked in red include high and very high temperatures. On 169th Julian day (June 28), zones with very high temperatures include District 21, District 22, neighborhoods 7 and 9, District 9, Airport neighborhoods, Fatah, Mehrabad Sarasiab, South Mehrabad, District 18, Khalij-e Fars Shomali neighborhoods, 17 Shahrivar, Imam Khomeini Shahrak, Hosseini-Ferdows, and District 19 of Aliabad neighborhood On this day, in District 22, except for neighborhoods 7 and 9, which have very high temperatures, and on the Shohadaye Khalij-e Fras Lake, which has a low temperature and a moderate temperature in a radius of about 1000 meters, other areas have high temperatures. Other areas with high temperatures include District 16, District 18, neighborhoods of Tolid-e Drau, Behdasht, Sahib al-Zaman, Yaftabad Shomail, Shadabad, Shamsabad, Khalij-e Fras Jonubi; District 19, neighborhoods of Ismail Abad, Dolatkhah, Nematabad, Ahmad Khomeini Shahrak,

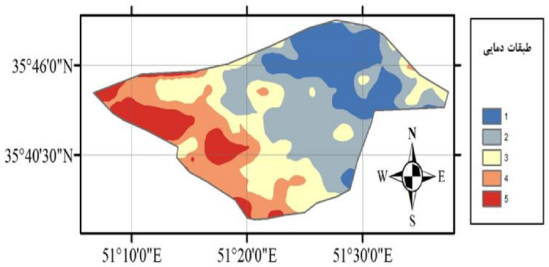

Figure 4. Spatial distribution of temperature zones in Tehran on 169th Julian day (June 18) 2017

[DOI: 10.32592/jorar.2022.14.1.2]

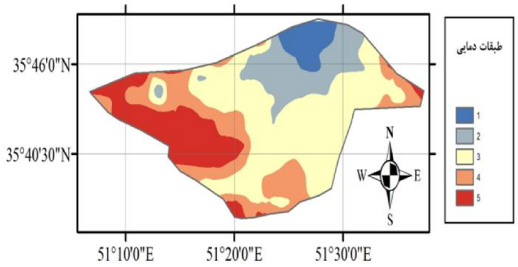

Figure 5. Spatial distribution of temperature zones in Tehran on 361st Julian day December 27, 2017

Khaniabad No Shomali and Jonubi, Esfandiari and Bostan, Qala-e-Morghi and Shariati Shomali and Jonubi; District 4, neighborhoods of Kuhsar and Hakimiyeh; District 5 neighborhoods of Ekbatan, Koy-e Bimeh, and Apadana Shahrak; District 12, neighborhoods Bazaar, Shahid Harandi and Takhti. On this day, the zones that have very low and low temperature include Districts 1 and 3; District 4, neighborhoods of Qasem Abad and Deh Narmak, Qanat-e Kowsar, Shemiran No, Valiasr Shahrak, Shian, and Lavizan, Mubarak Abad and Hossein Abad, Zarabkhaneh and Pasdaran, Shams Abad and Majidiyeh, Kazem Abad, Mehran; District 2, neighborhoods of Islamabad, Modiriyat, Darya, Derakhti, Shahrak-e Qarb, Ivanak; District 6, neighborhoods of Gandhi, Shiraz, Argentina-Saei, Yousefabad-Amirabad, Abbasabad, Meydan-e Jihad, Laleh Park, Fatemi, Abbasabad 6; District 7, neighborhoods of Niloufar-Shahid Ghandi and the northern half of neighborhoods of Kerman, Majidiyeh, and Dabestan-Majidiyeh.

In Figures 4 and 5, the zones marked in dark blue and blue represent the areas with very low and low temperatures, respectively. These clusters are most extensive and interconnected on 105th (April 26) and 361st Julian days (January 6). Accordingly, in the northern and eastern areas of Tehran, hot clusters located in these areas have been destroyed or weakened. According to the image on December 27, compared to the image on June 18, the heat island with very high temperature still remains on District 9, neighborhoods of Mehrabad airport; District 18, neighborhood of 17 Shahrivar, and the western part of District 21. On this day, in District 21, in the neighborhoods of Azadi Shahrak, Farhangian Shahrak, Tehransar Shomali and Markazi, the western half of Tehransar Qarbi, Pasdaran Shahrak, and Bashgah-e Naft, the temperature is changed from very high-to-high. Moreover, in Darya Shahrak, the temperature is changed from very high to the average, and in the western part of Tehransar Sharqi neighborhood, it has changed from very high-to-high and average. In district 22, neighborhoods of 7 and 9, the temperature was changed from very high-to-high. Furthermore, the temperature difference on Shohaday-e Khalij-e Fars Lake with its surroundings is imperceptible and expands to District 5 with moderate (average) temperature.

In District 9, the temperature in the neighborhoods of Mehrabad Jonubi and Sarasiab Mehrabad is changed from very high-to-high. Moreover, it is changed from high to moderate in the neighborhoods of Shahid Dastgheib, Imamzadeh Abdullah, Shamshiri, and the eastern half of Ostad Moein. In District 18, the cluster temperature in the neighborhoods of Khalij-e Fras Shomali, southern half of 17 Shahrivar, Imam Khomeini Shahrak, and western half Hosseini Ferdows is changed from very high-to-high. In addition, it is changed from high to moderate in the neighborhoods of Behdasht and Tolid-e Daru.

The temperatures in District 16, District 4 (neighborhoods of Kuhsar and Hakimiyeh), and District 5 (neighborhoods of Koy-e Bimeh, Apadana Shahrak, and the eastern half of Ekbatan Shahrak) have changed from high to moderate, high to moderate and low, as well as high to moderate, respectively. In addition, in District 2, a high-temperature cluster is observed in the neighborhoods of Azmaish Shahrak and Alstom.

Temporal changes in the intensity of the heat island in Tehran

Figure 3/1 shows the temporal changes in the heat island ratio in Tehran during 2017. Accordingly, from Julian days of 1 to 81 (January 12 to April 2) and 153 to 281 (June 12 to October 16), the intensity of the heat island of Tehran was higher than the average (about 0.067) for 210 days in a year as a result of changes in vegetation, climate, and air pollution.

Discussion and Conclusion

The method in the present study made it possible to identify the behavioral characteristics of urban temperature changes by pixel-based surface temperature separation with high spatial and temporal resolution; moreover, by obtaining spatial data analysis methods, local heat pattern was obtained. The diagram of periodic and

[DOI: 10.32592/jorar.2022.14.1.2]

irregular oscillations of heat islands in this study showed that the comparison of the spatial pattern of heat islands is not logical regardless of the time of location, and this issue has been ignored in many studies related to heat islands. Daily and weekly fluctuations in the intensity of the heat island and human exposure to it cause a wide range of diseases in humans. These diseases initiate from an unpleasant feeling and can lead to hypothermia, heat stroke, cardiovascular disease, respiratory disease, and eventually death by reducing the function of physical activity. Most deaths are observed in the elderly and those with respiratory illnesses; moreover, people with chronic illnesses, children, and people living in cold climates cannot easily tolerate the heat and are considered a vulnerable population. In most cases, the adverse effects and costs of health care can be reduced by identifying vulnerable people and applying management methods and appropriate measures. For at-risk population, treatment, medication, appropriate behavior in critical situations (organizational management and changes in work rules) is important to reduce the time of exposure to heat. Therefore, it is suggested that vulnerabilities are evaluated and cost-effective options are identified in the health sector due to the great effect of temperature on climatic conditions, air pollution, and human health, using the analytical method of daily surface temperature changes in this study.

Acknowledgments

The authors would like to express their gratitude to all those who contributed to the conduction of this research project.

Conflict of Interests

Authors declared no conflict of interests regarding the publication of the present study.

References

1. Landsberg HE. The Urban Climate. Academic Press, Maryland, 1981.
2. Hajizadeh M, Ramezani M, Hosseinshahi M. Investigating the effects of climate change on human health, SHEBAKMAG, 2019; 5(8): 51-56. [In Persian]
3. Sanagar E, Rafiyan M, Hanaee T, Monsefi D. The Effects of Urban Heat Islands Mitigation on Human Health through Change in Urban form Hot and Arid Climate of Mashhad, J. Env. Sci. Tech, 2020; 22(4). [In Persian].
4. Roth M, Oke TR, Emery WJ. Satellite derived urban heat islands from three coastal cities and the utilization of such data in urban climatology. International Journal of Remote Sensing. 1989; 10 (11): 1699-1720.
5. Gallo KP, Owen TW. Assessment of urban heat island: A multi-sensor perspective for the Dallas-Ft. Worth, USA region. Geocarto International, 1998; 13(4): 35-41.
6. Streutker DR. Satellite-measured growth of the urban heat island of Houston, Texas, Remote Sensing of Environment, 2003; 85: 282–289.
7. Lu D, Weng Q. Spectral mixture analysis of ASTER images for examining the relationship between urban thermal features and biophysical descriptors in Indianapolis, Indiana, USA. Remote Sensing of Environment, 2006; 104: 157–167.
8. Córdova K. Spatial Geotechnology applied to urban climate studies: Thermal analysis of urban surface and urban land use in Caracas city. 5th Urban Research Symposium 2009 http://www.meteo.fr/icuc9/presentations/GD/GD8-1.pdf.
9. Essa W, van der Kwast J, Verbeiren B, Batelaan O. (2013). Downscaling of thermal images over urban areas using the land surface temperature–impervious percentage relationship. Int. J. Appl. Earth Obs. Geoinf, 2013; 23(1): 95–108.
10. Sadeghinia A, Analysis of spatio-temporal structure of the urban heat island in Tehran through remote sensing and geographic information system. PhD Thesis on Climatology, Kharazmi University, Tehran, Iran, 2012. [In Persian].
11. Anselin L. Interactive techniques and exploratory spatial data analysis. In: Longley PA, Good child MF, Maguire DJ (Eds) Geographical information systems: principles, technical issues, management issues and applications. Wiley, New York, 1999; 253–266.
12. Mo X, Cheng C, Zhai F, Li H. Study on temporal and spatial variation of the urban heat island based on Landsat TM/ETM+ in central city and Binhai New Area of Tianjin, Multimedia Technology (ICMT), 2011 International Conference on. 26-28 July 2011; 4616-4622.
13. Xu H, Chen Y, Dan S, Qiu W. Spatial and temporal analysis of urban heat Island effects in Chengdu City by remote sensing. Geoinformatics, 19th International Conference, 2011; 1-5.